

Article

Using Principal Component Analysis (PCA) Combined with Multivariate Change-Point Analysis to Identify Brine Layers Based on the Geochemistry of the Core Sediment

Qiao Su ^{1,2} , Hongjun Yu ^{1,*}, Xingyong Xu ³, Bo Chen ¹, Lin Yang ¹, Tengfei Fu ^{1,2} , Wenquan Liu ^{1,2} and Guangquan Chen ^{1,2}

¹ Key Laboratory of Marine Sedimentology and Environmental Geology, First Institute of Oceanography, Ministry of Natural Resources, Qingdao 266061, China; suqiao@fio.org.cn (Q.S.) futengfei@fio.org.cn (T.F.)

² Laboratory for Marine Geology, Qingdao National Laboratory for Marine Science and Technology, Qingdao 266061, China

³ Guangxi Key Laboratory of Beibu Gulf Marine Resources, Environment and Sustainable Development, Fourth Institute of Oceanography, Ministry of Natural Resources, Beihai 536015, China; xuxingyong@fio.org.cn

* Correspondence: hjyu@fio.org.cn

Abstract: The underground brine in Southern Laizhou Bay is characterized by its large scale and high concentration, which can affect the distribution and migration of geochemical elements in sediments. Most studies on the brine are based on hydrochemical analysis, with little consideration being given from a geochemical perspective. Principal component analysis (PCA) is a powerful tool for discovering relationships among many elements and grouping samples in large geochemical datasets. However, even after reducing the dimensions through PCA, researchers still need to make judgments about the meaning represented by each principal component. Change-point analysis can effectively identify the points at which the statistical properties change in a dataset. PCA and change-point analysis have their respective advantages in the study of large sets of geochemical data. Based on the geochemical data of the LZ908 core, by combining these two methods, this study identified four elements (U, MgO, Br, and Na₂O) related to the action of seawater through PCA; then, multivariate change point analysis was conducted on these elements to detect the depths of different brine layers. The results of the analysis are basically consistent with those of other studies based on the water content, salinity, and other data, thus proving the effectiveness of this method. The combination of these two methods may also lead to novel approaches for related research.

Keywords: principal components analysis; change point analysis; underground brine; sediment geochemistry; southern Laizhou Bay



Citation: Su, Q.; Yu, H.; Xu, X.; Chen, B.; Yang, L.; Fu, T.; Liu, W.; Chen, G. Using Principal Component Analysis (PCA) Combined with Multivariate Change-Point Analysis to Identify Brine Layers Based on the Geochemistry of the Core Sediment. *Water* **2023**, *15*, 1926. <https://doi.org/10.3390/w15101926>

Academic Editor: Domenico Cichella

Received: 7 April 2023

Revised: 4 May 2023

Accepted: 16 May 2023

Published: 19 May 2023



Copyright: © 2023 by the authors. Licensee MDPI, Basel, Switzerland. This article is an open access article distributed under the terms and conditions of the Creative Commons Attribution (CC BY) license (<https://creativecommons.org/licenses/by/4.0/>).

1. Introduction

The global sea level has been fluctuating due to a variety of climatic changes since the Quaternary. In coastal areas, marine and terrestrial sediments have alternately formed, and time series of environmental evolutionary information are recorded in the sediments [1]. Intertidal zones are dynamic systems in which sediments are deposited by seawater or eroded by currents or wind, and they can be composed of mud and silt (mudflats), fine sand, or any mixture of these [2].

Brine is a significant source of table salt (NaCl) and other chemicals that are used in both domestic and industrial applications [3]. Southern Laizhou Bay is one of the main brine storage areas in China due to its wide distribution and high concentration of brine. The unique meteorological and hydrological conditions, as well as the ancient geographical environment and topographic features in southern Laizhou Bay, provide favorable conditions for the formation of brine [4]. Understanding the origin of salinity is

critical for improving salt production efficiency and providing advice for environmental protection [5]. The genesis and evolution of brine and saline groundwater have always been a challenge for geochemists and hydrogeologists [6]. The majority of studies on the origin of underground brine are based on hydrochemical analyses; however, numerous chemical and physical processes can alter the properties of underground brine, and almost all natural brines have experienced significant compositional changes compared to their initial state [7].

Sediment cores serve as fundamental raw data sources that offer novel research findings on the stratigraphic character, depositional history, and environmental shifts [8], thus reflecting the climatic conditions of brine formation [9]. The development of technology has enabled modern analytical instruments to gather more detailed geochemical datasets, thereby rendering the geochemical records of cores more complex and variable. Therefore, it has become more important to detect patterns and reduce noise in large geochemical datasets.

Early studies often used different ratio graphs or triangular graphs to interpret geochemical data [10]. Generally, the distribution of geochemical elements is caused by many geochemical processes that operate over a wide range of scales and typically interact with each other in multiple ways [11]. Nevertheless, multivariate datasets with more than three dimensions make such graphical techniques problematic [12].

Principal component analysis (PCA), a multivariate data analysis technology, can be used to extract most of the information from a sizable multi-dimensional data array into fewer dimensions. This method makes it possible to more quickly and quantitatively visualize a set of the re-expressed data [13], and it has been widely used with geochemical data to characterize geochemical trends and processes [1]. However, although PCA can delete redundant information between original variables to achieve the purpose of data dimensionality reduction, researchers still need to make subjective judgments about the meaning represented by each principal component.

Change-point detection can be used to accurately locate the places in a dataset where the statistical characteristics are changed, and it can be used to discover changes in the underlying model of a signal or time series [14]. By recasting geochemical records and classifying the issue as that of change-point detection, each change point is a moment at which a depth-series dataset is divided into two segments of self-consistent trends. In a typical case, the change-point method is more effective than other methods in detecting the trends of transitions in geochemistry [15].

PCA and change-point analysis have their respective advantages in studying large sets of geochemical data. Hence, by combining these two approaches, employing PCA to classify different combinations of elements, and subsequently conducting multivariate change-point analyses on the distinct element compositions, more comprehensive and superior analytical results can be obtained. This study attempts to combine these two methods to detect the depths of different brine layers by using geochemical data from the LZ908 drill core in Laizhou Bay.

2. Materials and Methods

2.1. Geological Settings and LZ908 Core

Southern Laizhou Bay is located in the Bohai Sea and northern Shandong Peninsula, China. Since the late Pleistocene, the Laizhou Bay area has experienced several transgressions, resulting in the formation of multiple layers of brine [6]. The presence of these brine layers has led to a more complex groundwater system than those in other regions, with intricate interactions among the seawater, groundwater, and brine [4]. Additionally, due to its location in the coastal region, it is also impacted by other factors such as hydrodynamic changes caused by the interaction between the land and the ocean [16]. The combination of these factors has resulted in an exceptionally complex pattern of the distribution of geochemical elements in the region [17].

The LZ908 core is located on the southern coast of Laizhou Bay ($37^{\circ}09' \text{ N}$, $118^{\circ}58' \text{ E}$; Figure 1). The drill core's site was originally located in Laizhou Bay, and it became land due to the reclamation of salt fields in the 1950s.

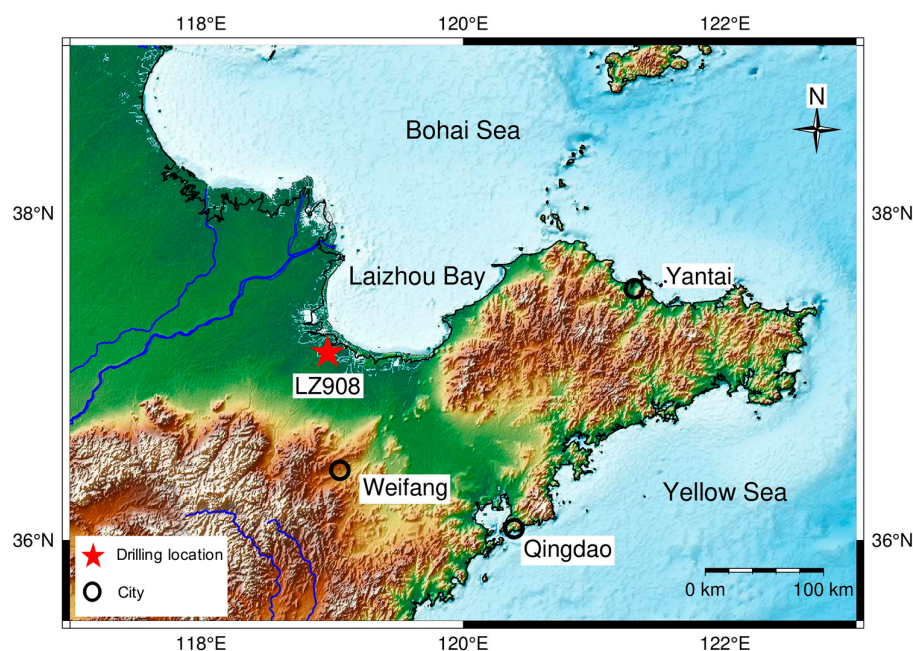


Figure 1. The location of borehole Lz908.

In the summer of 2007, the LZ908 core was drilled to a depth of 101.3 m by the First Institute of Oceanography, Ministry of Natural Resources, China. The core's diameter was 110 mm, and the average recovery rate reached 75%. After the core samples were extracted from the ground, they were immediately encapsulated in PVC tubes and transported to the laboratory for frozen storage.

The upper 54.3 m of the core mainly consisted of marine and coastal sediments, which are typically chosen for paleoclimatological and paleoenvironment studies, while the lower 47.0 m was classified as lacustrine and fluvial sediments [18].

2.2. Material

A total of 1063 samples were extracted from the core for geochemical analysis. The sampling densities were different according to the needs of the study, and the minimum interval was 2 cm. Of course, some samples in certain depths were missing due to the core sampling rate.

Geochemical analyses were carried out at the Institute of Earth Environment, Chinese Academy of Sciences. To minimize the impacts of large detrital particles on sediment compositions, the samples were dried and sieved through a standard 200 mesh sieve. Then, 0.6 g of a sieved sample was placed with 6 g of a mixed $\text{Li}_2\text{B}_4\text{O}_7$ and NH_4NO_3 flux into a platinum crucible, fused, and placed in a muffle furnace. The concentrations of major and trace elements were analyzed with a Philips PW4400 X-ray Fluorescence (XRF) spectrometer. Inductively coupled plasma–mass spectrometry (ICP-MS, Thermo Elemental, X Series, Thermo Fisher Scientific, Waltham, MA, USA) was used to determine 14 rare earth elements. There were a small amount of data below the detection threshold, and they were replaced with one-half of the detection limit [13].

After a thorough pretreatment method, the grain sizes of 2141 samples at different depths were tested with a Malvern Mastersizer 2000. The water content and salt content were only tested in the upper 60 m of the LZ908 core.

Furthermore, calcium carbonate, minerals, mineralization, micropaleontology, minerals, and color reflectance were separately tested, and these data and related research results can provide references.

2.3. Principal Component Analysis (PCA)

PCA can reduce the intricacy of multidimensional data while preserving the trends and patterns of raw data. It accomplishes this by transforming the data into smaller dimensions, and these serve as feature summaries [19]. PCA may determine correlations between the investigated geochemical parameters, thus characterizing the depositional environment [20].

Early in 1992, Meglen systematically summarized the application of the PCA method in the chemical domain (including data processing, the PCA frame, and the interpretation of results) [21]. The importance of the use of PCA in solving a geochemical question was later discussed by Ariyibi et al. [22]; since then, PCA has been more and more widely applied in geochemistry [23]. In this study, we constructed PCA with the open platform of R language, and the variables were normalized before PCA [13].

2.4. Multivariate Data Change-Point Analysis

An observation sequence is often described as a series of discrete, non-overlapping segments, each of which corresponds to a different event and has distinct characteristics of its trajectory. If the temporal bounds of those segments are determined, insightful information from homogeneous phases can be retrieved [24]. Change-point detection addresses the problem of estimating the point at which the statistical properties of an observation sequence change. As longer datasets are gathered, an increasing number of applications require the detection of changes in the distributional features of such datasets [25].

In order to systematize an enormous amount of work, Truong et al. (2020) offered a selective survey of algorithms for the offline detection of numerous change points in multivariate time series [14]. Fortunately, the majority of the detection methods described in their study are accessible in the Python language via the module of *ruptures* [24], which is the most comprehensive change-point detection library to date. The multivariate change-point analysis of geochemical data in this study was mainly based on the *rupture* packages.

3. Results

3.1. General Characteristics of Chemical Elements

The concentrations of 34 chemical elements in the LZ908 core were determined in our study (Figure 2). The contents of major elements in the sediments ranged from 68.37 wt% to 97.16 wt%. SiO₂ was the most prevalent major element, ranging in abundance from 27.6 wt% to 75.0 wt%. The content of Al₂O₃ was relatively stable, ranging between 6.65 wt% and 18.14 wt%, while that of CaO varied greatly from 0.61 wt% to 25.56 wt%. The maximum contents of Fe₂O₃, MgO, Na₂O, and K₂O were less than 10 wt%, while the maximum contents of P₂O₅ and TiO₂ were less than 1 wt% and 0.4 wt%, respectively. The lowest content of a major element was MnO, and the maximum value was only 0.24 wt%.

Regarding other elements, the average concentrations of Zr, Sr, and Ba were several hundred ppm, while V, Cr, Br, Ce, Zn, Rb, Ni, La, and Nd had concentrations of several tens of ppm, and the remaining elements all had concentrations of less than 20 ppm.

According to the correlations between chemical elements (Figure 3), they could be divided into several groups. The largest group was dominated by Al₂O₃ and Fe₂O₃, and it included K₂O, TiO₂, V, Cr, Nd, Zn, Rb, Ni, Co, Ga, Nb, Sc, and Th. The correlation coefficient between Al₂O₃ and Fe₂O₃ exceeded 0.89, and the correlation coefficients among the elements in the group were also relatively high.

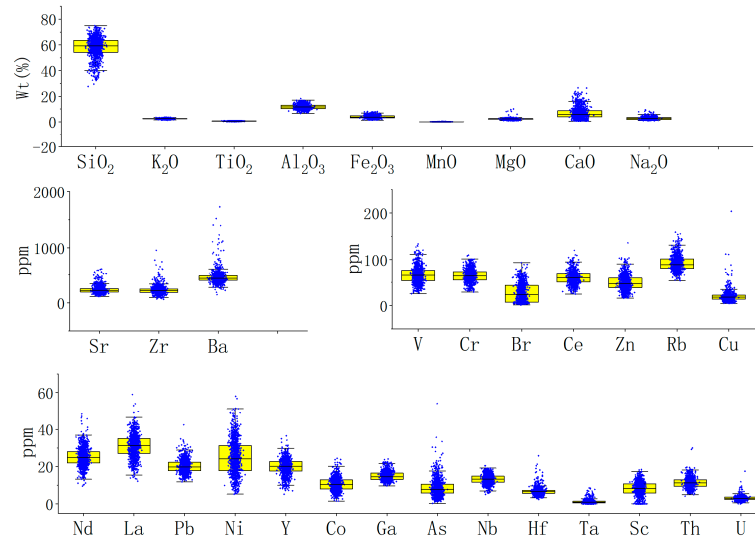


Figure 2. General statistical characteristics of elements.

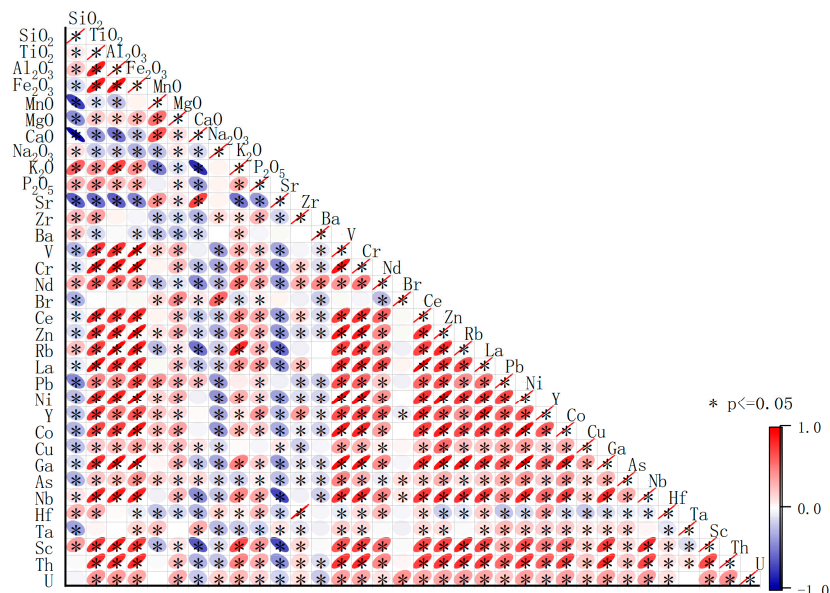


Figure 3. Correlation heat map of chemical elements.

CaO, Sr, MnO, and SiO₂ formed a group. CaO, Sr, and MnO were positively correlated with each other, while SiO₂ was negatively correlated with them. The strongest correlation coefficient was between Zr and Hf, and it was more than 0.99. These two elements had very low correlation coefficients with other elements, which allowed them to create a distinct group. Similarly, Na₂O and Br had a correlation coefficient of about 0.59, while the correlation coefficients between them with all of the other elements were all below 0.5, with most being below 0.1.

There were also strong positive correlations among La, Ce, and Y, but their correlation coefficients with some other elements were also rather high. P₂O₅, Cu, As, Ba, and Ta all had weak correlations with other elements.

3.2. PCA of Geochemistry

Principal component extraction was carried out on a data matrix consisting of 1063 sediment samples with 34 chemical variables that were determined. There are several methods for determining how many principal components to use, and a scree plot, in

which variances are arranged from largest to smallest, is particularly intuitively appealing. A scree plot depicts the amount of variance explained by the 34 principal components (Figure 4). The scree plot suggested that five principal components were sufficient. The first five principal components accounted for 14.6, 4.94, 2.94, 2.25, and 1.66 of the overall variance, which were about 43%, 15%, 9%, 7%, and 5% of the total variance, respectively. The cumulative variances of these five principal components cumulative variances reached 78%.

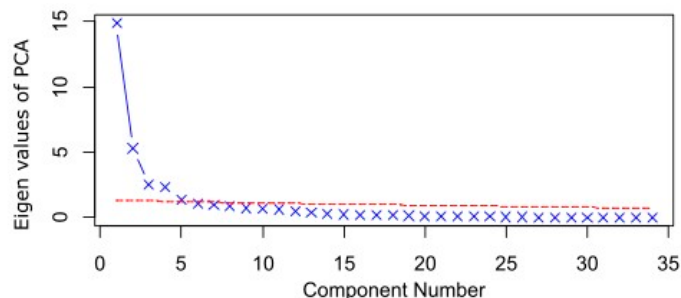


Figure 4. Scree plot of the PCA.

The relative variable loadings on the first five principal components are depicted in Figure 5. Horizontal bars represent the loadings' magnitudes for each variable. The first principle component included Fe₂O₃, Ni, Ga, Zn, V, Cr, Al₂O₃, Co, La, Ce, TiO₂, Rb, Nb, Th, Sc, Y, Pb, and Nd, and they were all positively correlated. The second principle component was mainly composed of inverse relationships with K₂O, SiO₂, CaO, and Sr, as well as a positive relationship with MnO. The third principle component included Hf and Zr, and they were both positively correlated. The fourth principle component consisted of a positive relationship with U, MgO, Br, and Na₂O. The fifth principle component consisted of a negative relationship with As and a positive relationship with Ba. In addition, the variables with a correlation of less than 0.5 contained Cu, P₂O₅, and Ta.

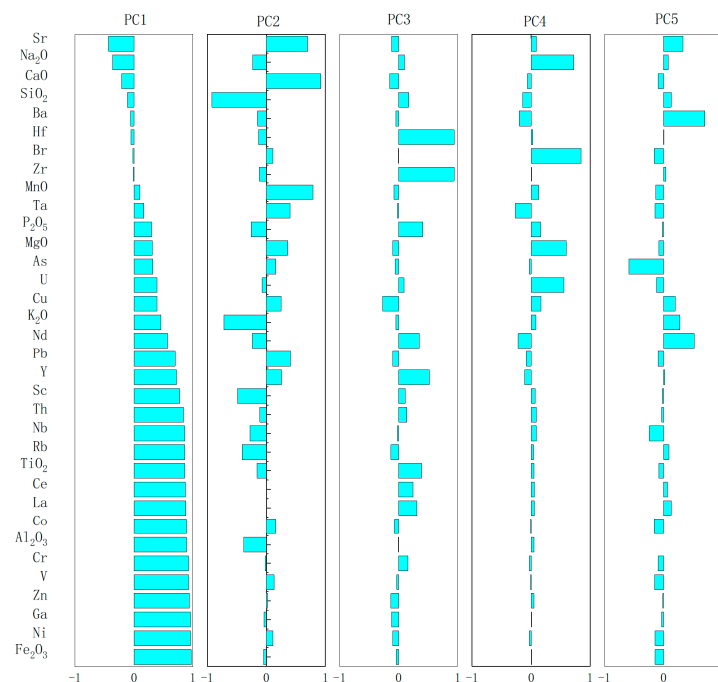


Figure 5. Principal component loadings for geochemistry data.

3.3. Multivariate Change-Point Analysis

According to the results of the PCA, each principal component represented a different number of variables. Multivariate change-point analysis was performed on the elements contained in each principal component based on the *ruptures* package, and the results are shown in Figure 6. An alternation of gray and yellow indicates that there was a change point.

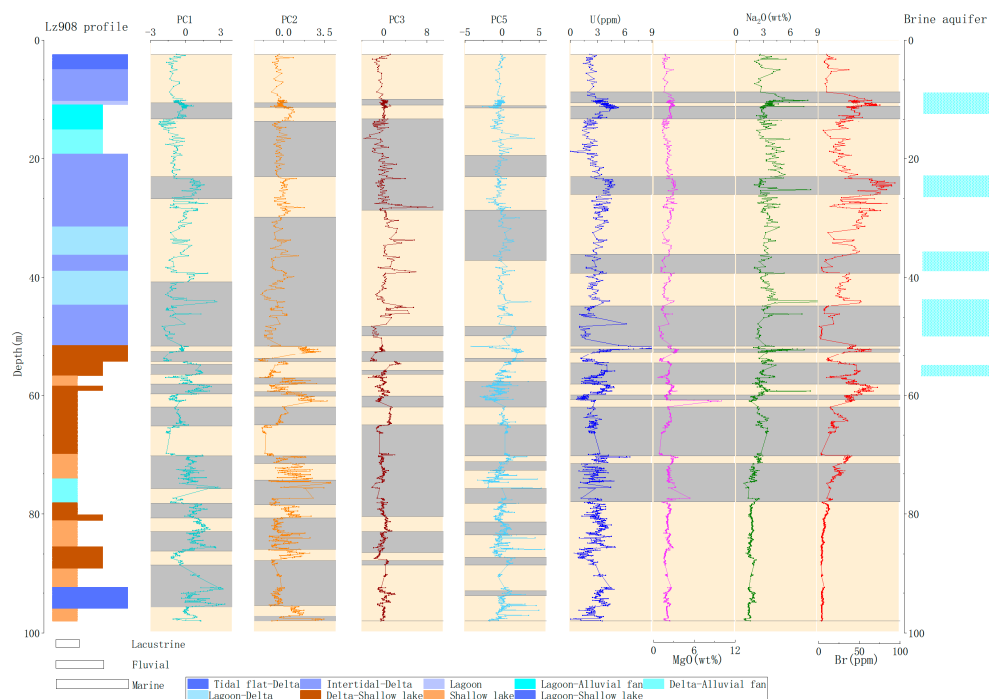


Figure 6. Results of the multivariate change-point analysis.

The multivariate change-point results of PC4 were largely compatible with the distribution of the brine layer in the upper 60 m of the LZ908 core, as determined using various approaches; specific details are provided in Section 4.

4. Discussion

Source matter, including clastic material, dissolved material, and organic material, makes up the original materials that form sediments. The source matter mainly comes from the weathering of the parent rock. Various types of parent rock lead to various weathering products, and even the same type of parent rock can produce different weathering products due to varying weathering conditions. In general, the provenance of sediments is the major factor controlling the geochemistry of sediments, although it can be greatly modified using subsequent processes. The depositional environment, which is mostly governed by the subsidence rate, will determine the chemical changes during the deposition. Chemical and biochemical processes controlling element solubilities in seawater, submarine weathering, and redox conditions are also important for particular types of sediment [26].

Coastal sediments form archives that are widely used by environmental geochemists [27]. In the process of the evolution of sediments from source to sink, it is generally believed that the influence of grain size exceeds the influence of all other control factors on the changes in sediment's chemical composition [28]. Therefore, the sediment grain size is a potent indicator used in numerous paleoenvironmental studies. There are strong associations between some geochemical characteristics of the core and changes in grain size, which suggests that sediment sorting has a significant impact on the geochemical parameters. As such, it is essential to take the impact of sediment grain size into account when analyzing geochemical indicators [29]. Yi et al. systematically analyzed the grain size of the LZ908 core, and they concluded that grain size variation is an indicator of the Asian monsoon

intensity, which is primarily driven by both solar insolation (major) and global ice volume (minor) forcing [30]. Furthermore, by using regression and stringent verification techniques, the reference water table could be rebuilt from the sediment grain size [31], and the depth of the brine was closely related to changes in trace element contents [32].

According to a previous study, grain size is the most important factor for controlling the distribution of elements in the study area [33]. To compare the relationship between the element concentration and grain size of different samples, we first standardized the concentration values of each element to a range of 0–1. According to the ratios of standardized element concentration values to the median grain size (Figure 7), most elements in PC1 had a relatively high correlation coefficient (shown in red), which showed that the elements in PC1 were mainly controlled by grain size changes. In addition, PC1 contained the most elements of the biggest group based on the correlation coefficients between the elements (Figure 3). Specifically, K_2O had relatively high correlation coefficients with some elements in PC1, while its correlation with grain size was very low. The absence of K_2O from PC1 further suggested that the distribution of K_2O was influenced by an influence other than grain size.

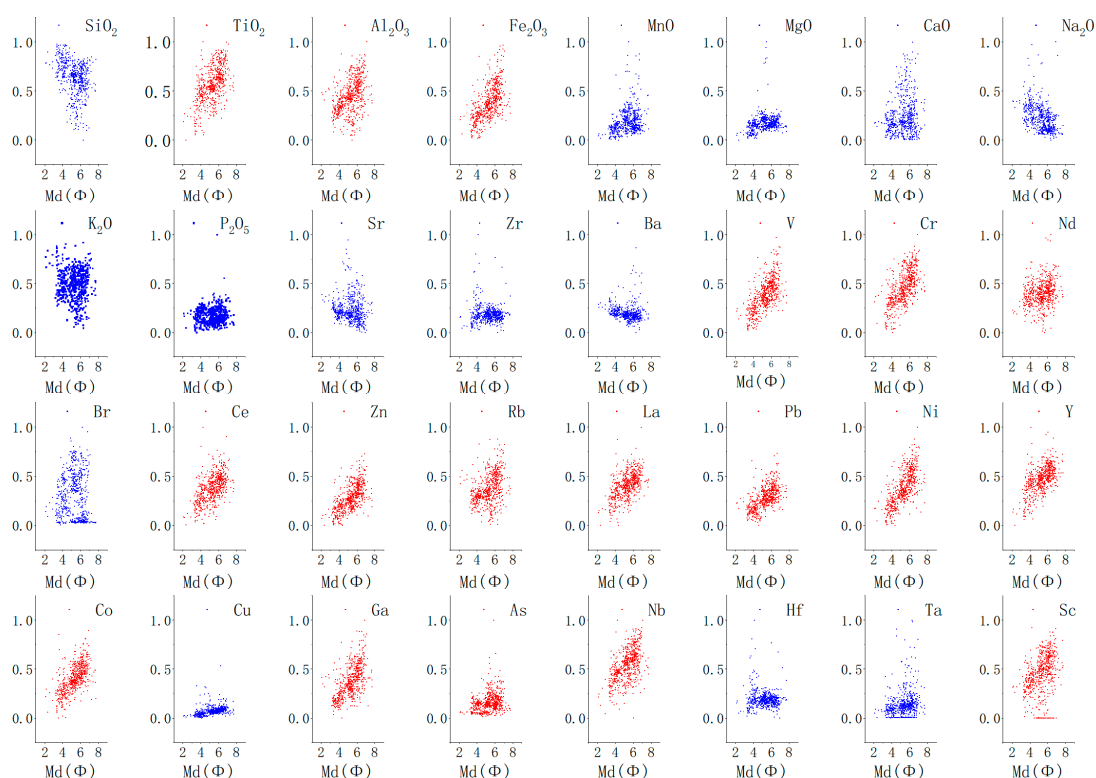


Figure 7. Ratios of the elements' concentrations (standardized) to the median grain size.

The biogeochemical processes and physical processes in coastal zones are coupled on multiple scales. The forms and functions of interactions among sediment microbes, animals, plants, and abiotic elements in intertidal environments are complicated and uncertain. However, there is no doubt that biogeochemistry can change the sedimentary environment, thereby affecting the distribution of elements in sediments (Fusi, M. et al., 2022 [34]).

Ca and Sr are significant constituents of marine biota constituents and exert considerable effects on the oceanic biogeochemical cycle [35]. K is a crucial component for all living organisms, and its enrichments can be produced by some kind of biological pumping [36]. In delta and estuarine areas, K can become ionic due to biogenic transformation [37]. The content of Si can also be affected by the dilution of biological components, and high SiO_2 content may be related to the presence of more biogenic silica [38]. The development of

subsurface anoxic conditions in sediments is promoted by a high rate of organic matter accumulation, and this will eventually result in the active redox recycling of Mn [39]. Therefore, each element in PC2 was related to the biogeochemical cycle, and PC2 could represent the biological action of chemical elements.

In PC2, CaO, SiO₂, Sr, and MnO had a high correlation with each other, and the correlation coefficients between K₂O and them were 0.79, 0.62, 0.53, and 0.48, respectively. K₂O had a higher correlation coefficient with Rb than with any other element, and it reached 0.80. In addition, K₂O also had relatively high correlation coefficients with Fe₂O₃ and Sc. According to the results of the PCA, although grain size and other factors can also affect the distribution of K₂O, biological action plays a major role.

According to earlier research, trace elements such as Hf and Zr are usually useful for determining the provenance of sediment because they are refractory and have low mobility during weathering and transportation processes [40]. PC3 only included Hf and Zr, which may have been related to sediment provenance. Additionally, the correlation coefficient of Zr and Hf, which was larger than 0.99, also supported this idea.

Sediments rich in biogenic opal have the highest Ba levels because diatom frustules can contain up to 30,000 ppm of Ba. Therefore, Ba is usually used as the most common nutrient element for estimating the primary productivity [41]. Likewise, more and more evidence shows that natural organic matter strongly interacts with As, affecting its speciation and migration in various aquatic environments [42]. PC5, which contained Ba and As, may be related to marine primary productivity.

Based on the data on sediment water content, Yao et al. have identified the potential brine-enriched layers in the upper 60 m of the LZ908 core [17]. In this study, additional tests on the sediment salinity of the upper 60 m of the LZ908 core were performed, and they were combined with the other tested data and findings from previous studies; thus, the upper 60 m of the LZ908 core was divided into five brine layers (Figure 8). These brine layers were all formed during the transgression period [43], indicating that the salinity originated from seawater. According to Figure 6, the results of the multivariate change-point analysis of the elements in PC4 were very close to the brine layer distribution.

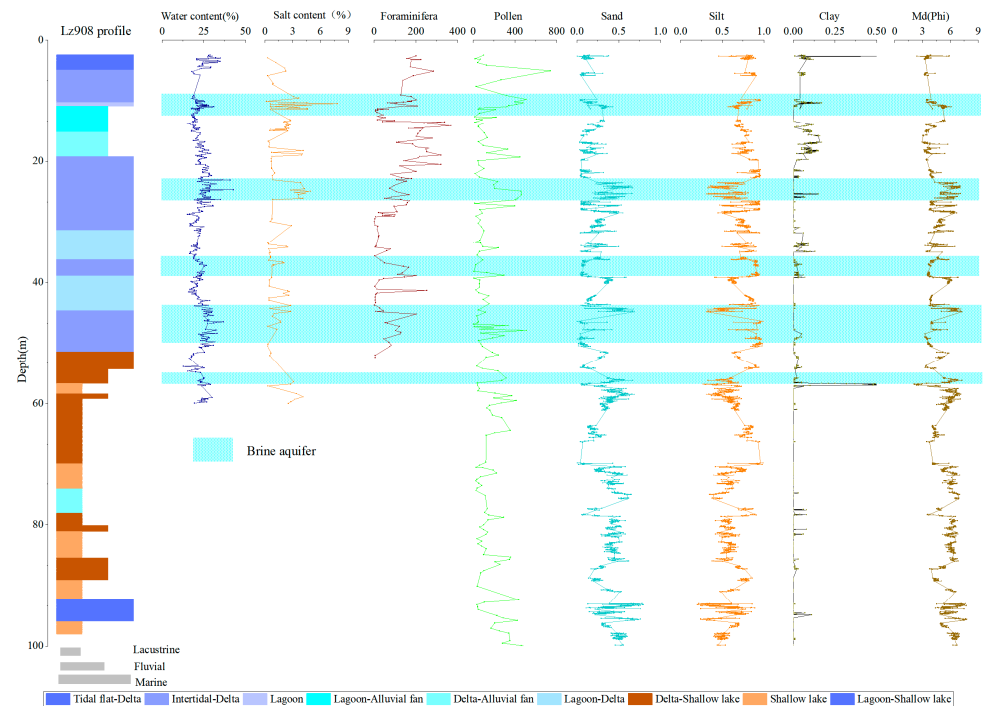


Figure 8. Profile and brine layer distribution of the LZ908 core.

Geochemical elements are affected by several factors, such as the stratigraphic structure, material source, weathering conditions, element reactions at the water–sediment interface, the nature of the sedimentary environment, and the diagenesis process [11]. Due to the location of the coastal zone and the existence of several brine layers, the sediments in Laizhou Bay are affected by more factors than in other areas; thus, the distribution of elements in the sediments is more complicated. Although the deposition and enrichment of many elements in sediments are influenced by seawater, the results of the PCA and multivariate change-point analysis indicated that U, MgO, Br, and Na₂O were more significantly affected.

As a chemically conserved halogen element, Br hardly ever takes part in any diagenetic reactions [16]. In nature, Br is mainly concentrated in seawater in the form of ions, and the biggest natural reservoir is the ocean [44]. Br has historically been utilized in combination with Cl as a geochemical indicator for seawater intrusion in coastal regions and alone as a paleosalinity proxy and stratigraphic marker in cores [45].

It is widely known that seawater has substantially higher salinity than that of freshwater; therefore, its two most common cation constituents, Na and Mg, have historically been employed as proxies for marine effects in salt marsh systems [46,47]. Brine–rock interactions are important events in the mineralizing process throughout the path of brine flow. During extensive fluid–rock interactions, the composition of the brine significantly changes from its original state, which is essential for the efficient mobilization of U and Br [48].

Therefore, the elements U, MgO, Br, and Na₂O in PC4 exhibited a more pronounced response to seawater compared to other elements, providing further evidence of the close relationship between PC4 and brine. Among all of the elements, Br had the highest correlation coefficients with Na₂O, MgO, and U, which were 0.58, 0.46, and 0.42, respectively. The highest correlation coefficient of Na₂O was also related to Br, and its correlation coefficients with other elements were less than 0.42. The correlation coefficient between MgO and MnO was the highest, reaching 0.56, followed by that with Br. The correlation between U and all other elements was very low—not higher than 0.42.

It is still debatable how the brine in Laizhou Bay was generated. The majority of researchers came to the conclusion that the brine in Laizhou Bay is the result of seawater evaporation, while some studies suggested that frozen brine existed [49]. What is certain is that different concentration paths of seawater can affect the properties of brine [50], and the assemblages of minerals that form, the order in which they precipitate, and their relative abundances are all determined by the relative composition of ionic species in the original brine [51]. For example, during the freezing process, Na is first precipitated in the form of mirabilite at a seawater concentration factor of 4, followed by halite with a concentration factor of about 10. During the evaporation process, Na only precipitates in the form of hydrohalite at a concentration factor of about 10 [50,52].

Furthermore, the complex exchange among groundwater, seawater, and brine in the Laizhou Bay area, coupled with the water–rock exchange, also has an important influence on the element distribution [53]. Ca and/or Mg (cations) in groundwater may have a direct cation exchange with Na (cation) in the clay layer near the coastline of Laizhou Bay [54]. Cation exchange plays an essential role in the change in the contents of Na and Mg [55]. Changes in the compositions of water and sediment can also lead to significant variations in the behavior of U [56].

According to the distribution of elements in PC4, the characteristics of the elements varied among different layers. The first layer of brine exhibited relatively high levels of all elements, while the second layer only showed a lower concentration of Na₂O. However, the trends in element content in other layers were not discernible. The phenomenon in which element contents decreases with the increase in burial depth exists in many sediments, especially for Br. This change is most probably due to diagenetic reactions that release Br from the sediment into the pore waters, with the released Br migrating upwards and being lost from the sediment [57].

5. Conclusions

Principal component extraction was carried out on the geochemical data of the LZ908 core, and the scree plot suggested that five principal components were sufficient, the cumulative variances of which reached 78%. The first principle component included Fe₂O₃, Ni, Ga, Zn, V, Cr, Al₂O₃, Co, La, Ce, TiO₂, Rb, Nb, Th, Sc, Y, Pb, and Nd. Most elements in PC1 had a relatively high correlation coefficient with the median grain size, which showed that the elements in PC1 were mainly controlled by grain size changes.

K₂O, SiO₂, CaO, Sr, and MnO made up the second principle component, and these elements were all related to the biogeochemical cycle, which illustrated that PC2 can represent the biological action of chemical elements. The third principle component included Hf and Zr, and the correlation coefficient between them was also the highest among all elements. Hf and Zr are usually useful for determining the provenance of sediments; therefore, PC3 may be related to sediment provenance.

The fourth principle component consisted of U, MgO, Br, and Na₂O, which exhibited a more pronounced response to seawater compared to other elements, providing evidence of the close relationship between PC4 and seawater. The fifth principle component included As and Ba, and both of these elements are the representative of marine primary productivity.

Then, multivariate change-point analysis was performed on the elements in every principal component with the *ruptures* package, and the result showed that PC4 was consistent with the distribution of the brine layer. This result is in agreement with the influence of seawater on the elements of the sediments in PC4.

Reducing the dimensionality of elements through principal component analysis and then using multivariate change-point analysis to identify potential change points provides an effective and more convenient method for identifying brine layers, indicating that the combination of these two methods is successful. This also offers a novel approach for similar studies.

Author Contributions: Conceptualization, Q.S. and H.Y.; methodology, Q.S. and X.X.; software, B.C. and L.Y.; validation, Q.S. and H.Y.; formal analysis, Q.S., T.F. and W.L.; investigation, Q.S. and G.C.; resources, Q.S.; data curation, Q.S.; writing—original draft preparation, Q.S.; writing—review and editing, H.Y.; visualization, B.C. and L.Y.; supervision, X.X.; project administration, H.Y.; funding acquisition, Q.S. All authors have read and agreed to the published version of the manuscript.

Funding: This research was funded by the Basic Scientific Fund for National Public Research Institutes of China (GY0220Q03), the National Natural Science Foundation of China (42176213;42276223), and the Shandong Natural Science Foundation (ZR2020MD078).

Data Availability Statement: The data used in this paper are available from the corresponding author upon reasonable request.

Acknowledgments: The authors give their most sincere thanks to the reviewers for their contributions to the improvement of this article and are also grateful for the support of “observation and research station of seawater intrusion and soil salinization, Laizhou Bay”.

Conflicts of Interest: The authors declare no conflict of interest.

References

1. Jia, C.; Yang, F.; Liu, S.; Wang, C.; Chang, W. Paleoclimatic interpretation in southern Laizhou Bay since the late Pleistocene: Evidence from groundwater and sedimentary strata. *Cont. Shelf Res.* **2022**, *237*, 104676. [[CrossRef](#)]
2. Stal, L.J. Coastal Sediments: Transition from Land to Sea. In *The Marine Microbiome*; Springer International Publishing: Cham, Switzerland, 2016; pp. 283–304. ISBN 3319329987; 9783319329987.
3. Ene, G.E.; Okogbue, C.O.; Chigoziri, O.J. Extraction constraints and environmental significance of brine discharges in the Asu River watershed, Southeastern Nigeria. *Environ. Earth Sci.* **2018**, *77*, 402. [[CrossRef](#)]
4. Liu, S.; Tang, Z.; Gao, M.; Hou, G. Evolutionary process of saline-water intrusion in Holocene and Late Pleistocene groundwater in southern Laizhou Bay. *Sci. Total. Environ.* **2017**, *607–608*, 586–599. [[CrossRef](#)] [[PubMed](#)]
5. Du, Y.; Ma, T.; Chen, L.; Xiao, C.; Liu, C. Chlorine isotopic constraint on contrastive genesis of representative coastal and inland shallow brine in China. *J. Geochem. Explor.* **2016**, *170*, 21–29. [[CrossRef](#)]

6. Liu, J.; Wang, H.; Wang, F.; Qiu, J.; Saito, Y.; Lu, J.; Zhou, L.; Xu, G.; Du, X.; Chen, Q. Sedimentary evolution during the last ~1.9 Ma near the western margin of the modern Bohai Sea. *Palaeogeogr. Palaeoclimatol. Palaeoecol.* **2016**, *451*, 84–96. [[CrossRef](#)]
7. Gerber, C.; Vaikm, E.R.; Aeschbach, W.; Babre, A.; Jiang, W.; Leuenberger, M.; Lu, Z.-T.; Mokrik, R.; Müller, P.; Raidla, V.; et al. Using 81Kr and Noble Gases to Characterize and Date Groundwater and Brines in the Baltic Artesian Basin on the One-Million-Year Timescale. *Geochim. Cosmochim. Acta* **2017**, *205*, 187–210. [[CrossRef](#)]
8. Nair, M.P.; Akhil, P.S.; Sujatha, C.H. Geochemistry of Core Sediment from Antarctic Region. *Res. J. Chem. Environ.* **2013**, *17*, 8–12.
9. Roy, P.D.; Nagar, Y.C.; Juyal, N.; Smykatz-Kloss, W.; Singhvi, A. Geochemical signatures of Late Holocene paleo-hydrological changes from Phulera and Pokharan saline playas near the eastern and western margins of the Thar Desert, India. *J. Asian Earth Sci.* **2009**, *34*, 275–286. [[CrossRef](#)]
10. Batayneh, A.; Zumlot, T. Multivariate Statistical Approach to Geochemical Methods in Water Quality Factor Identification; Application to the Shallow Aquifer System of the Yarmouk Basin of North Jordan. *Res. J. Environ. Earth Sci.* **2012**, *4*, 756–768.
11. Abdelwahab El-Sayed, S.; Hassan, H.B.; El-Sabagh, M.E.I. Geochemistry and mineralogy of Qaroun Lake and relevant drain sediments, El-Fayoum, Egypt. *J. Afr. Earth Sci.* **2022**, *185*, 104388. [[CrossRef](#)]
12. Iwamori, H.; Yoshida, K.; Nakamura, H.; Kuwatani, T.; Hamada, M.; Haraguchi, S.; Ueki, K. Classification of geochemical data based on multivariate statistical analyses: Complementary roles of cluster, principal component, and independent component analyses. *Geochem. Geophys. Geosys.* **2017**, *18*, 994–1012. [[CrossRef](#)]
13. Xue, J.; Lee, C.; Wakeham, S.G.; Armstrong, R.A. Using principal components analysis (PCA) with cluster analysis to study the organic geochemistry of sinking particles in the ocean. *Org. Geochem.* **2011**, *42*, 356–367. [[CrossRef](#)]
14. Truong, C.; Oudre, L.; Vayatis, N. Selective review of offline change point detection methods. *Signal. Process.* **2020**, *167*, 107299. [[CrossRef](#)]
15. Davis, A.C. Segmenting geochemical records using hierarchical probabilistic models. *Chem. Geol.* **2021**, *559*, 119973. [[CrossRef](#)]
16. Du, Y.; Ma, T.; Chen, L.; Shan, H.; Xiao, C.; Lu, Y.; Liu, C.; Cai, H. Genesis of salinized groundwater in Quaternary aquifer system of coastal plain, Laizhou Bay, China: Geochemical evidences, especially from bromine stable isotope. *Appl. Geochem.* **2015**, *59*, 155–165. [[CrossRef](#)]
17. Yao, J.; Yu, H.J.; Xu, X.Y.; Yi, L.; Su, Q. Deposition characteristics in brine aquifers and brine formation in Laizhou Bay area. *Adv. Mar. Sci.* **2010**, *28*, 473–477. (In Chinese)
18. Yi, L.; Deng, C.; Xu, X.; Yu, H.; Qiang, X.; Jiang, X.; Chen, Y.; Su, Q.; Chen, G.; Li, P.; et al. Paleo-megalake termination in the Quaternary: Paleomagnetic and water-level evidence from south Bohai Sea, China. *Sediment. Geol.* **2015**, *319*, 1–12. [[CrossRef](#)]
19. Abdi, H.; Williams, L.J. Principal component analysis. *Wiley Interdiscip. Rev. Comput. Stat.* **2010**, *2*, 433–459. [[CrossRef](#)]
20. Garcia, R.J.L.; Da Silva Júnior, J.B.; Abreu, I.M.; Soares, S.A.R.; Araujo, R.G.O.; de Souza, E.S.; Ribeiro, H.J.S.; Hadlich, G.M.; Queiroz, A.F.D.S. Application of PCA and HCA in geochemical parameters to distinguish depositional paleoenvironments from source rocks. *J. S. Am. Earth Sci.* **2020**, *103*, 102734. [[CrossRef](#)]
21. Meglen, R.R. Examining large databases: A chemometric approach using principal component analysis. *Mar. Chem.* **1992**, *39*, 217–237. [[CrossRef](#)]
22. Ariyibi, E.A.; Folami, S.L.; Ako, B.D.; Ajayi, T.R.; Adelusi, A.O. Application of the principal component analysis on geochemical data: A case study in the basement complex of Southern Ilesa area, Nigeria. *Arab. J. Geosci.* **2011**, *4*, 239–247. [[CrossRef](#)]
23. Sönmez, F.N.; Kockar, S.; Yilmaz, H. Efficiency of singularity and PCA mapping of mineralization-related geochemical anomalies: A comparative study using BLEND and <180 µm stream sediment geochemical data. *Bull. Miner. Res. Explor.* **2022**, *168*, 11–33. [[CrossRef](#)]
24. Truong, C.; Oudre, L.; Vayatis, N. ruptures: Change point detection in Python. *arXiv* **2018**, arXiv:1801.00826.
25. Killick, R.; Eckley, I.A. Changepoint: An R Package for Changepoint Analysis. *J. Stat. Softw.* **2014**, *58*, 1–15. [[CrossRef](#)]
26. Rollinson, H.R. *Using Geochemical Data: Evaluation, Presentation, Interpretation*; Longman Scientific & Technical: London, UK, 1993; ISBN 9781315845548. [[CrossRef](#)]
27. Semenkova, I.N.; Konyushkova, M.V.; Heidari, A.; Nikolaev, E. Chemical differentiation of recent fine-textured soils on the Caspian Sea coast: A case study in Golestan (Iran) and Dagestan (Russia). *Quat. Int.* **2021**, *590*, 48–55. [[CrossRef](#)]
28. von Eynatten, H.; Tolosana-Delgado, R.; Karius, V.; Bachmann, K.; Caracciolo, L. Sediment generation in humid Mediterranean setting: Grain-size and source-rock control on sediment geochemistry and mineralogy (Sila Massif, Calabria). *Sediment. Geol.* **2016**, *336*, 68–80. [[CrossRef](#)]
29. Huang, X.; Mei, X.; Yang, S.; Zhang, X.; Li, F.; Hohl, S.V. Disentangling Combined Effects of Sediment Sorting, Provenance, and Chemical Weathering From a Pliocene-Pleistocene Sedimentary Core (CSDP-1) in the South Yellow Sea. *Geochem. Geophys. Geosystems* **2021**, *22*, e2020GC009569. [[CrossRef](#)]
30. Yi, L.; Yu, H.; Ortiz, J.D.; Xu, X.Y.; Chen, S.L.; Ge, J.Y.; Hao, Q.Z.; Yao, J.; Shi, X.F.; Peng, S.Z. Late Quaternary linkage of sedimentary records to three astronomical rhythms and the Asian monsoon, inferred from a coastal borehole in the south Bohai Sea, China. *Palaeogeogr. Palaeoclimatol. Palaeoecol.* **2012**, *329–330*, 101–117. [[CrossRef](#)]
31. Yi, L.; Yu, H.; Ortiz, J.D.; Xu, X.; Qiang, X.; Huang, H.; Shi, X.; Deng, C. A reconstruction of late Pleistocene relative sea level in the south Bohai Sea, China, based on sediment grain-size analysis. *Sediment. Geol.* **2012**, *281*, 88–100. [[CrossRef](#)]
32. Holser, W.T.; Burns, R.G. Trace elements and isotopes in evaporites. *Mineral. Soc. Am. Short. Course Notes* **1979**, *6*, 295–346.
33. Hongxia, W.; Xianjun, Z.; Xianhong, L.; Zhixun, Z.; Zhenhong, L.; Guangtao, Z. Geochemistry Characteristics of Sediment and Provenance Relations of Sediments in Core NT1 of the South Yellow Sea. *J. China Univ. Geosci.* **2007**, *18*, 287–298. [[CrossRef](#)]

34. Fusi, M.; Booth, J.M.; Marasco, R.; Merlino, G.; Garcias-Bonet, N.; Barozzi, A.; Garuglieri, E.; Mbobbo, T.; Diele, K.; Duarte, C.M.; et al. Bioturbation Intensity Modifies the Sediment Microbiome and Biochemistry and Supports Plant Growth in an Arid Mangrove System. *Microbiol. Spectr.* **2022**, *10*, e01117-22. [[CrossRef](#)]
35. Zhou, H.; Peng, X.; Pan, J. Distribution, source and enrichment of some chemical elements in sediments of the Pearl River Estuary, China. *Cont. Shelf Res.* **2004**, *24*, 1857–1875. [[CrossRef](#)]
36. Mangelsdorf, P.J.; Wilson, T.R.; Daniell, E. Potassium enrichments in interstitial waters of recent marine sediments. *Science* **1969**, *165*, 171–174. [[CrossRef](#)]
37. Sukhija, B.S.; Varma, V.N.; Nagabhushanam, P.; Reddy, D.V. Differentiation of palaeomarine and modern seawater intruded salinities in coastal groundwaters (of Karaikal and Tanjavur, India) based on inorganic chemistry, organic biomarker fingerprints and radiocarbon dating. *J. Hydrol.* **1996**, *174*, 173–201. [[CrossRef](#)]
38. Norton, S.A.; Bienert, R.W.; Binford, M.W.; Kahl, J.S. Stratigraphy of total metals in PIRLA sediment cores. *J. Paleolimnol.* **1992**, *7*, 191–214. [[CrossRef](#)]
39. Calvert, S.E.; Pedersen, T.F.; Pasava, J. Sedimentary geochemistry of manganese; implications for the environment of formation of manganiferous black shales. *Econ. Geol. Bull. Soc. Econ. Geol.* **1996**, *91*, 36–47. [[CrossRef](#)]
40. Liu, J.; Zhu, Z.; Xiang, R.; Cao, L.; He, W.; Liu, S.; Shi, X. Geochemistry of core sediments along the Active Channel, northeastern Indian Ocean over the past 50,000 years: Sources and climatic implications. *Palaeogeogr. Palaeoclimatol. Palaeoecol.* **2019**, *521*, 151–160. [[CrossRef](#)]
41. Liang, H.; Xu, G.; Xu, F.; Yu, Q.; Liang, J.; Wang, D. Paleoenvironmental evolution and organic matter accumulation in an oxygen-enriched lacustrine basin: A case study from the Laizhou Bay Sag, southern Bohai Sea (China). *Int. J. Coal Geol.* **2020**, *217*, 103318. [[CrossRef](#)]
42. Wang, S.; Mulligan, C.N. Effect of natural organic matter on arsenic release from soils and sediments into groundwater. *Environ. Geochem. Health* **2006**, *28*, 197–214. [[CrossRef](#)]
43. Yi, L.; Lai, Z.; Yu, H.; Xu, X.; Su, Q.; Yao, J.; Wang, X.; Shi, X. Chronologies of sedimentary changes in the south Bohai Sea, China: Constraints from luminescence and radiocarbon dating. *Boreas* **2013**, *42*, 267–284. [[CrossRef](#)]
44. Vainikka, P.; Hupa, M. Review on bromine in solid fuels. Part 1: Natural occurrence. *Fuel* **2012**, *95*, 1–14. [[CrossRef](#)]
45. Moreno, J.; Fatela, F.; Leorri, E.; Moreno, F.; Freitas, M.; Valente, T.; Araújo, M.; Gómez-Navarro, J.; Guise, L.; Blake, W. Bromine soil/sediment enrichment in tidal salt marshes as a potential indicator of climate changes driven by solar activity: New insights from W coast Portuguese estuaries. *Sci. Total. Environ.* **2017**, *580*, 324–338. [[CrossRef](#)] [[PubMed](#)]
46. Millero, F.J. *Chemical Oceanography*; Elsevier: Amsterdam, The Netherlands, 2016.
47. Chague-Goff, C.; Dawson, S.; Goff, J.R.; Zachariasen, J.; Berryman, K.; Garnett, D.; Waldron, H.; Mildenhall, D. A tsunami (ca. 6300 years BP) and other Holocene environmental changes, northern Hawke's Bay, New Zealand. *Sediment. Geol.* **2002**, *150*, 89–102. [[CrossRef](#)]
48. Richard, A.; Boulvais, P.; Mercadier, J.; Boiron, M.-C.; Cathelineau, M.; Cuney, M.; France-Lanord, C. From evaporated seawater to uranium-mineralizing brines: Isotopic and trace element study of quartz–dolomite veins in the Athabasca system. *Geochim. Cosmochim. Acta* **2013**, *113*, 38–59. [[CrossRef](#)]
49. Hu, F.; Xu, X.; Liang, J.; Yang, C.; Huang, M.; Su, Q. Machine learning-based seawater concentration pathway prediction. *Comput. Electr. Eng.* **2021**, *94*, 107336. [[CrossRef](#)]
50. Herut, B.; Starinsky, A.; Katz, A.; Bein, A. The role of seawater freezing in the formation of subsurface brines. *Geochim. Cosmochim. Acta* **1990**, *54*, 13–21. [[CrossRef](#)]
51. Getenet, M.; Garcia-Ruiz, J.M.; Otalora, F.; Emmerling, F.; Al-Sabbagh, D.; Verdugo-Escamilla, C. A Comprehensive Methodology for Monitoring Evaporitic Mineral Precipitation and Hydrochemical Evolution of Saline Lakes: The Case of Lake Magadi Soda Brine (East African Rift Valley, Kenya). *Cryst. Growth Des.* **2022**, *22*, 2307–2317. [[CrossRef](#)]
52. Starinsky, A.; Katz, A. The formation of natural cryogenic brines. *Geochim. Cosmochim. Acta* **2003**, *67*, 1475–1484. [[CrossRef](#)]
53. Chang, Y.; Hu, B.X.; Xu, Z.; Li, X.; Tong, J.; Chen, L.; Zhang, H.; Miao, J.; Liu, H.; Ma, Z. Numerical simulation of seawater intrusion to coastal aquifers and brine water/freshwater interaction in south coast of Laizhou Bay, China. *J. Contam. Hydrol.* **2018**, *215*, 1–10. [[CrossRef](#)]
54. Han, D.M.; Song, X.F.; Currell, M.J.; Yang, J.; Xiao, G. Chemical and isotopic constraints on evolution of groundwater salinization in the coastal plain aquifer of Laizhou Bay, China. *J. Hydrol.* **2014**, *508*, 12–27. [[CrossRef](#)]
55. Sabarathinam, C.; Bhandary, H.; Ali, A. Strategies to characterize the geochemical interrelationship between coastal saline groundwater and seawater. *Environ. Earth Sci.* **2021**, *80*, 642. [[CrossRef](#)]
56. Tiwari, R.K.; Dalai, T.K.; Samanta, S.; Rahaman, W.; Singh, S.K.; Horner, T.J. Geochemistry of uranium in the Ganga (Hooghly) River estuary, India: The role of processes in the water column and below the sediment-water interface. *Mar. Chem.* **2022**, *247*, 1–13. [[CrossRef](#)]
57. Price, N.B.; Calvert, S.E. The contrasting geochemical behaviours of iodine and bromine in recent sediments from the Namibian shelf. *Geochim. Cosmochim. Acta* **1977**, *41*, 1769–1775. [[CrossRef](#)]

Disclaimer/Publisher's Note: The statements, opinions and data contained in all publications are solely those of the individual author(s) and contributor(s) and not of MDPI and/or the editor(s). MDPI and/or the editor(s) disclaim responsibility for any injury to people or property resulting from any ideas, methods, instructions or products referred to in the content.